World Academy of Science, Engineering and Technology
International Journal of Chemical and Materials Engineering
Vol:15, No:6, 2021

Operational Challenges of Marine Fiber Reinforced Polymer Composite Structures Coupled with Piezoelectric Transducers

H. Ucar, U. Aridogan

***Abstract*—**Composite structures become intriguing for the design of aerospace, automotive and marine applications due to weight reduction, corrosion resistance and radar signature reduction demands and requirements. Studies on piezoelectric ceramic transducers (PZT) for diagnostics and health monitoring have gained attention for their sensing capabilities, however PZT structures are prone to fail in case of heavy operational loads. In this paper, we develop a piezo-based Glass Fiber Reinforced Polymer (GFRP) composite finite element (FE) model, validate with experimental setup, and identify the applicability and limitations of PZTs for a marine application. A case study is conducted to assess the piezo-based sensing capabilities in a representative marine composite structure. A FE model of the composite structure combined with PZT patches is developed, afterwards the response and functionality are investigated according to the sea conditions. Results of this study clearly indicate the blockers and critical aspects towards industrialization and wide-range use of PZTs for marine composite applications.

***Keywords*—**FRP, marine composite, piezoelectric transducer, sea state, wave-induced loads.

I. Introduction

IN the evolving industrial market, there have been numerous ongoing research and development projects for novel materials in terms of mechanical performance, endurance and cost. Within this scope, interest in composite materials has been arisen since they can have different properties due to their various ingredients [1], [2]. One of the most commonly used composite materials is Fiber Reinforced Polymer (FRP). FRP is a composite made from a polymer matrix that is bonded with natural fiber which reinforces the material and provides strength and stiffness to the composite. FRP composites have an important advantage in replacing metals due to their low weight. Additionally, they offer high corrosion resistance and durability as well as low maintenance cost. Due to these reasons, FRP composite structures are widely used in marine and aerospace applications.

In the last four decades, piezoelectric materials with their inherent capability to transform mechanical strain energy to electrical energy have gained attention to be used for health monitoring purposes [3]-[5]. These materials can also be used as actuators according to the inverse piezoelectric effects, inducing an expansion of the ceramic via an electric field [6]. In the last century, many types of piezoelectric materials have been evolved over the past century. The most widely used of these are PZT. PZTs have been extensively used in sensors and actuators due to their direct coupling and their capability to output large voltages [7]. There have been numerous studies investigating the applicability of PZTs as actuators or sensors. However, most of the studies have focused on cantilever beams, clamped plates or disks for the sake of easiness. Dragasius et al. [8] used the piezoelectric sensors for health monitoring in a composite plate. Presas et al. [9] studied the use of PZT patches for submerged disk to determine the frequency response functions. Larson et al. [10] investigated the active vibration control performance with piezoelectric actuators installed to B-1B aircraft fuselage in a laboratory environment. Their studies showed that vibration levels at the fuselage skin could be significantly suppressed in all simulated flight phases. For the investigation of possible usage in an automotive environment, Song et al. [11] conducted experiments for active vibration control with piezoelectric actuators and sensors on a half-scaled passenger vehicle. Their experimental results show that the vibration and noise can be lowered effectively using piezoelectric actuators and sensors.

Even though there are massive number of articles addressing the proof-of-concept usage of PZTs for aerospace and automotive applications, the possible proof-of-concept usage in naval structures and critical aspects for the real-life applications have been not widely studied.

This study focuses on the applicability of PZTs integrated to a complex marine structure, such as GFRP composite marine hull subjected to hydrodynamic loads. First, a simple piezo-based experimental GFRP composite beam model was created in order to identify the characteristic properties of the GFRP material to be used in the numerical study. After the numerical model was verified by the experimental study, the hull of a boat having a displacement of 10 tones was modeled numerically and the applicability of PZTs on the hull was investigated under the specified sea-state condition.

II. Piezo-Based GFRP Beam Study

A. Experimental Setup

On the purpose of identifying the mechanical characteristics of GFRP composite material and validating the electromechanical coupling model, an experimental cantilever beam set-up having a dimension of 500x50x1 mm (LxWxD) was built and a PZT patch was embedded at the clamped side

H. Ucar, was with Koc University, Istanbul, Turkey (corresponding author, phone: +90-532-467-7997; e-mail: hkucar@gmail.com).
U. Aridogan, was with Koc University, Istanbul, Turkey (e-mail: aridogan@gmail.com).

of the beam. In this part of the study, using the inverse piezoelectric effect, the structure was excited by the embedded PZT patch and the response was measured at the tip via Laser Doppler Vibrometer (LDV). The experimental setup and measurement system are shown in Figs. 1 and 2, respectively.

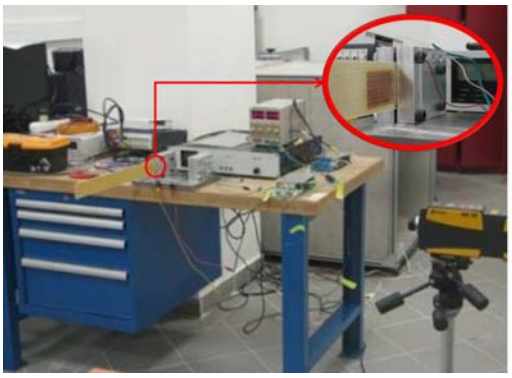

Fig. 1 Experimental Setup

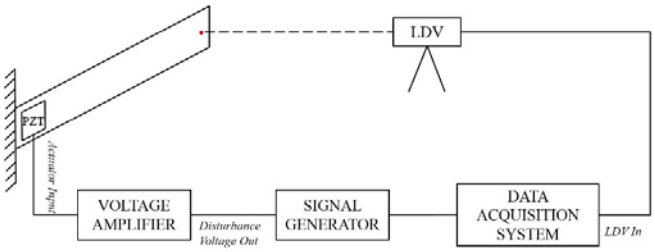

Fig. 2 Measurement System

Physical, material and electromechanical properties of PZT patch (PI Dura-act 876.A12) are provided by the manufacturer for the used material (PIC 255) and presented in Table I.

TABLE I
PHYSICAL, MATERIAL AND ELECTROMECHANICAL PROPERTIES OF THE PZT PATCH

Property	PZT Patch (PIC255)
Length (mm)	65
Width (mm)	31
Thickness (mm)	0.5
Elastic Modulus (GPa)	70.2
Poisson's Ratio	0.36
Density (kg/m^3)	7800
Operating Voltage (V)	-100 to +400
Relative Permittivity,	
σ_{33}^T/σ_0	1750
σ_{11}^T/σ_0	1650
Piezoelectric Voltage Coefficient, g_{31}, (10^{-3} Vm/N)	-11.3

TABLE II
NATURAL FREQUENCIES OF THE COMPOSITE BEAM

Mode Number	Frequency (Hz)	Amplitude (dB)
1	3.2	23.2
2	19.2	27
3	50.7	23.1

The natural frequencies of the system were determined from the frequency response measured at the tip of the beam. Accordingly, with reference to the frequency response, first three natural frequencies of the system are given in Table II.

B. System Identification of GFRP Composite

According to Euler Beam Theory, the differential equation for the lateral vibration of beams is derived from the shear and bending moments acting on the elements of the beam, as shown in (1) [12]:

$$EI\frac{d^4y}{dx^4}-\rho\omega^2 y=0 \tag{1}$$

where EI is the flexural rigidity, ρ is the mass per unit length of the beam and ω is the natural frequency of the beam. The natural frequencies are found from (1) to be

$$\omega_n=\beta_n^2\sqrt{\frac{EI}{\rho}}=(\beta_n l)^2\sqrt{\frac{EI}{\rho l^4}} \tag{2}$$

where the number β_n depends on the boundary conditions and l is the length of the beam.

By using the measured frequency response of the structure, the damping factor of the GFRP composite was aimed to be estimated. For this purpose, Peak-Amplitude Method, one of the modal parameter estimation methods, was used [13]. In this method, the frequency of the maximum amplitude, A_{max} as well as the the frequencies at where the amplitudes are $A_{max}/\sqrt{2}$ are selected and for each mode n, (3) has to be performed.

$$\zeta_n\cong\frac{\omega_a-\omega_b}{2\omega_n} \tag{3}$$

where ω_n is the natural frequency at which the peak amplitude occurs, ω_a and ω_b are the half-power points. Using (2) and (3) with respect to the measured frequency responses, the elastic modulus and damping ratio of the GFRP composite beam were derived as in Table III.

TABLE III
ELASTIC PROPERTIES OF GFRP COMPOSITE

Elastic Modulus (GPa)	Damping Ratio
45	0.0228

C. FE Modeling and Validation

After identifying the mechanical characteristics of the GFRP composite, the numerical composite model was created by using the obtained material parameters. PZT material properties were modelled as anisotropic to expose the dynamic behavior of the piezoelectric material accurately. As in the experimental study, PZT patch was used as an actuator and the frequency response of the system was determined at the tip of the beam and compared with the experimental result. The numerical model and frequency response of the structure were shown in Figs. 3 and 4, respectively.

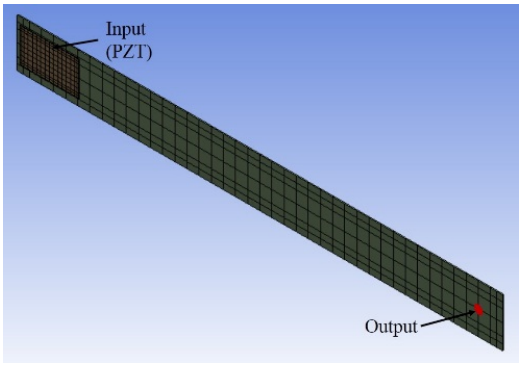

Fig. 3 Numerical Model of GFRP Composite Beam

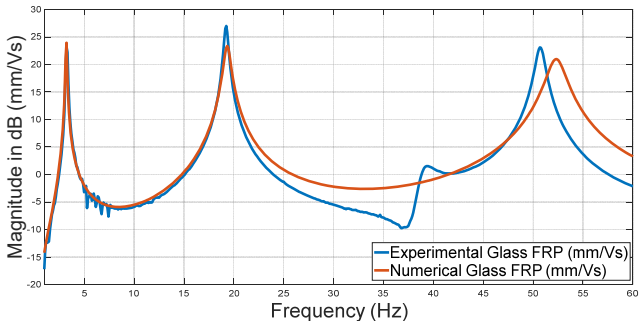

Fig. 4 Frequency Responses at Tip of GFRP Composite Beam

As shown in Fig. 4, it can be seen that the numerical frequency response agrees reasonably well with the experimentally measured one. Note that around 38 Hz, there is a "bump" in the experimental result because of the constraint at the clamped side of the beam. This effect was not included in the numerical study because it is not noteworthy. Consequently, it can be stated that the numerical model of composite structure coupled with PZT patch is valid and the piezoelectric and composite material characteristics are quite accurately defined to be used for a complex model.

III. Electromechanical Composite Hull Study

A. Ship Modeling

In order to study the applicability of PZT patches on a marine composite structure, a 16 m composite boat was utilized as the structural model basis. The general characteristics of the boat are presented in Table III and the FEM model is shown in Fig. 5. For the sake of easiness and the computational cost reduction, the hull of the boat was considered.

TABLE IV
General Hull Characteristics

Length	16 m
Width	3 m
Displacement	10 tons
Draft	0.80 m
Thickness of Hull	0.02 m
Freeboard	1.64 m
Material	GFRP

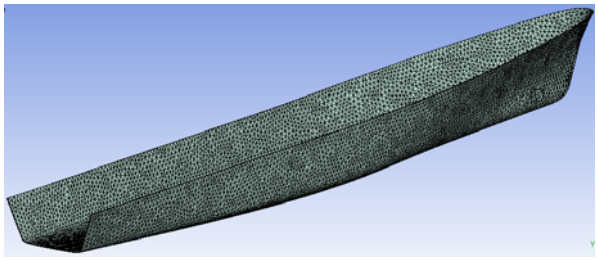

Fig. 5 FE Model of Hull

Point masses were properly distributed along the hull. This point mass distribution includes the payload, lightship mass and the fluid mass on board. In this study, 4 PZT patches (PI Dura-act 876.A12) were located at the port side of the bow of the ship, as shown in Fig. 6. In order to investigate the effect of wave-induced loads on submerged surfaces, 2 of the PZT patches were placed below the waterline while the others were placed above the waterline. Contrary to the GFRP beam study described in previous section, the direct effect of the piezoelectricity was considered in this case and the electrical potential output was of interest.

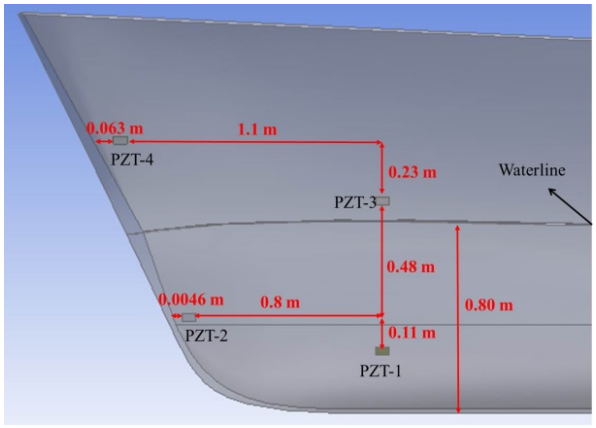

Fig. 6 Locations of PZT Patches

For the numerical study, it is critical to assign proper boundary conditions. Otherwise, high restraint forces and other factors may lead to false results in the analysis [14]. For sagging and hogging load cases, the rigid body motion constraints were applied at the bow and stern locations, as illustrated in Fig. 7.

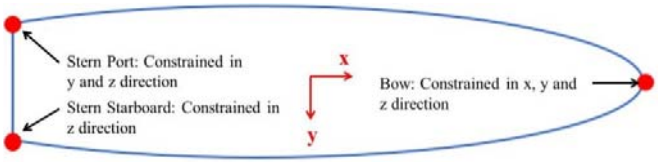

Fig. 7 Boundary Constraints [14]

B. Sea-State Loads

One of the most common sources for the generation of hull vibrations is wave-induced forces which strongly depend on the sea-states [15]. The sea-states are defined by the World Meteorological Organization (WMO) standard sea-state code

(Douglas Scale) and given in Table V for the East Mediterranean Sea [16].

TABLE V
SEA-STATES FOR EAST MEDITERRANEAN SEA (UP TO 6)

Sea-State	Modal Wave Period (s)	Mean Values of Significant Wave Height (m)
0-1	4.42	0.05
2	5	0.30
3	6.25	0.88
4	8.15	1.88
5	10.16	3.25
6	11.74	5

Irregular waves can be defined mathematically using spectrum formulas that have different formulations throughout the research. One of these spectrum formulations was recommended by the 12th International Towing Tank Conference (ITTC) and defined in terms of modal wave period and significant wave height, as shown in (4) and (5) [17].

$$S(\omega) = \frac{A}{\omega^5} e^{-\left(\frac{B}{\omega^4}\right)} \tag{4}$$

where ω is the wave frequency in radians per second, A and B are constants given in (5)

$$A = 488\frac{H_{1/3}^2}{T_m^4}\ ,\ B = \frac{1949}{T_m^4} \tag{5}$$

where $H_{1/3}$ is the significant wave height and T_m is the modal wave period. This sea spectrum is unidirectional and applicable for the long-crested irregular waves [18]. By using the spectrum, the long-crested wave surfaces can be derived for a specified time, as shown in Fig. 8.

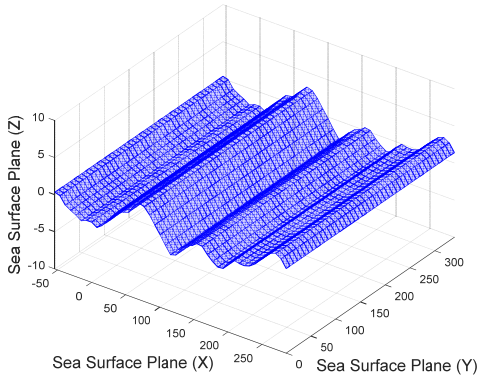

Fig. 8 Long-Crested Irregular Wave at the Spatial Domain

IV. RESULTS AND DISCUSSION

In order to investigate the applicability and functionality of piezoelectric materials on a GFRP composite hull, the aforementioned spectral wave-induced loads were applied as the harmonic excitations to the wetted surface of the ship model for sea-state 6 and the behavior of PZT patches coupled with the hull under this load was determined.

The strain fields for the port side of the bow are presented in Fig. 9 for the selected frequencies. Note that the locations of the PZT patches are shown in the figure with black rectangles. Besides, the resultant displacements of the PZT patch locations and the voltage outputs are displayed in Figs. 10 and 11, respectively.

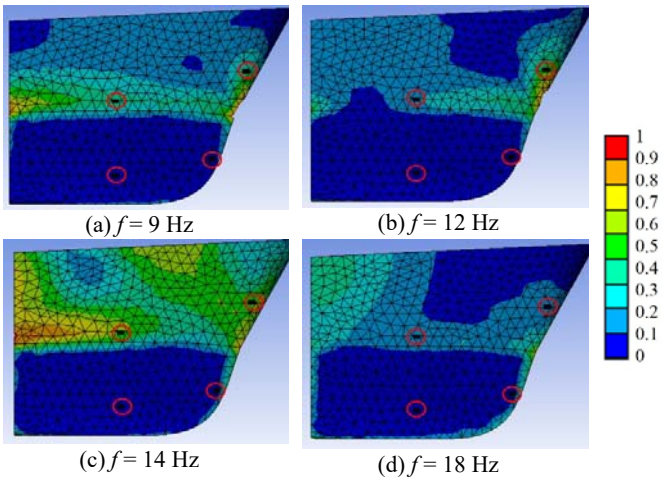

Fig. 9 Normalized Strain Field at Port Side of Bow

As shown in Figs. 9 and 11, the structure, at where PZT-1 and 2 are located, exhibits rigid body behavior. In the structure showing rigid behavior, very small strain values are obtained. It has been determined that voltage outputs cannot be generated in PZT-1 and 2, located below the waterline. When the equivalent strain and displacement values in the locations of the mentioned PZTs are examined, it is clear that the structure exhibits a rigid body behavior. Surfaces coupled with water behave as rigid bodies since they act in unison with the water mass, excited by the wave-induced loads. Therefore, it is considered that the wave-induced loads are not effective in generating voltage for the wetted surfaces. However, it has been observed that high voltage outputs, up to breakdown value of piezoelectric material, PIC255, can be produced in PZT patches mounted on surfaces above the waterline. Especially, PZT-4, which is placed close to the constraint at the bow of the ship, has been determined to be the one with the highest voltage output due to the high strain values.

TABLE VI
SENSING CAPABILITY AND BREAKAGE RISK LEVELS OF PZTS LOCATED AT PORT SIDE)

PZT #	Position w.r.t. Waterline	PZT Sensing Capability	PZT Breakage Risk Level
PZT-1	Below	Low	Low
PZT-2	Below	Low	Low
PZT-3	Above	High	Medium
PZT-4	Above	High	High

Table VI presents an overview for the location, sensing capability and breakage risk of PZT patches. The preferred location is PZT-3 location due to the fact the sensing capability is high whereas the breaking risk can be considered as medium. This “medium risk” means that the detailed

investigation for different static and dynamic loading is still required to mitigate the possible breakage risks.

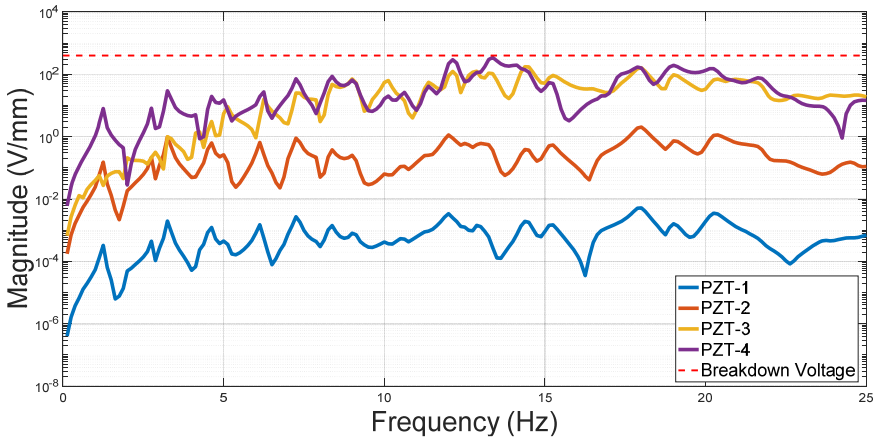

Fig. 10 Voltage Outputs at PZT Locations

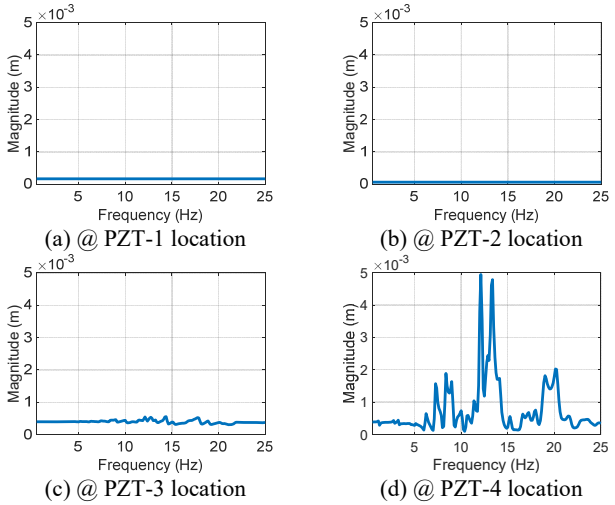

(a) @ PZT-1 location (b) @ PZT-2 location

(c) @ PZT-3 location (d) @ PZT-4 location

Fig. 11 Displacement at PZT Locations

V. Conclusion

In this study, the applicability of piezoelectricity through with direct effects such as energy harvesting and sensing properties, on a GFRP composite hull was investigated by means of embedded PZT patches. In order to establish a validated electromechanical composite model, a GFRP composite beam embedded with PZT patches was built. First, mechanical characteristics of the composite material were determined via experimentally measured frequency responses on the beam. By using the obtained parameters, the numerical composite beam model was created and validated with the experimental results. Having verified model parameters for coupled piezoelectric and composite material, a valid GFRP composite hull model coupled with PZT patches was created. A total of 4 PZT patches were embedded on the port side of the bow. Wave-induced loads, one of the common forces that the hull is subjected to, were applied to the hull model from port bow side for the Sea-State 6 in the Mediterranean Sea and the efficiency of the PZT patches was evaluated with the obtained voltage outputs.

Once the obtained results were studied, it was determined that voltage outputs could not be obtained from the PZT patches below the waterline, while a satisfactory amount of voltage output could be obtained from other PZT patches. Wetted surfaces coupled with water exhibit rigid behavior with the water mass when exposed to waves, therefore no displacement is observed on the surface and voltage cannot be generated by PZT patches. As far as the wave-induced loads for the excitation are concerned, it can be stated that it would be appropriate not to place PZT patches on the surfaces below the waterline and to investigate the strain field of the structure based on the wave encounter frequencies primarily, then to place patches on the surfaces above the waterline as close to the constraints as possible.

In this study, only long-crested waves at sea-state 6 were considered and the functionality of the PZTs was investigated. In the future study, it is aimed to study the behavior of PZTs with changing sea-state conditions. Besides, short-crested waves will be taken into consideration as the operational load acting on the hull and energy harvesting will also be carried out under the circumstances where PZTs are applicable with the appropriate sea-states.

Acknowledgment

The experimental setup was developed, and the experiments were carried out during authors' academic study at Koç University. The authors gratefully acknowledge the in-kind support from Professor İpek Başdoğan (Koç University) for the experiment setup and Yonca-Onuk Shipyard JV for composite structures.

References

[1] A.C. Corbin, B. Sala, D. Soulat, M. Ferreira, A.R. Labanieh, V. Placet, "Development of quasi-unidirectional fabrics with hemp fiber: A competitive reinforcement for composite materials" *J. Compos. Mater.,* 2020.

[2] M. Montemurro, M.I. Izzi, J. El-Yagoubi, D. Fanteria, "Least-weight composite plates with unconventional stacking sequences: Design,

analysis and experiments" *J. Compos. Mater.,* 2019, 53, pp. 2209–2227.
[3] Z.L. Wang and J. Song. "Piezoelectric nanogenerators based on zinc oxide nanowire arrays" *Science,* 2006, 312, 242–6
[4] S.R. Anton and H.A. Sodano, "A review of power harvesting using piezoelectric materials" *Smart Mater. Struct.*, 2007, 16 R1–R21, pp. 2003-2006.
[5] U. Aridogan, I. Basdogan, A.Ertürk, "Analytical modeling and experimental validation of a structurally integrated piezoelectric energy harvester on a thin plate" *Smart Mater. Struct.*, 2014, 23, pp. 533-547.
[6] A. Preumont, *Vibration Control of Active Structures*, Kluwer Academic Publishers, 1997
[7] M. Safaei, H.A. Sodano, S.R. Anton, "A review of energy harvesting using piexoelectric materilas: state-of-the-art a decade later (2008-2018)" *Smart Mater. Struct.*, 2019, 28, (62 pp).
[8] E. Dragasius, D. Eiduknynas, V. Jurenas, D. Mazeika, M. Galdikas, A. Mystkowski, J. Mystkowska, "Piezoeletric transducer-based diagnostic system for composite structure health monitoring" *Sensors*, 2021,21,253.
[9] A. Presas, D. Valentin, E. Egusquiza, C. Valero, M. Egusquiza, M. Bossio, "Accurate determination of the frequency response function of submerged and confined structures by using PT patches" *Sensors*, 2017, 17, 660.
[10] Larson, C.R., et al., Piezoceramic active vibration suppression control system development for the B-1B aircraft. Proceedings of SPIE, 1998. 3326: p. 294-305.
[11] Song, C.K., et al., Active vibration control for structural-acoustic coupling system of a 3-D vehicle cabin model. Journal of Sound and Vibration, 2003. 267(4): p. 851-865.
[12] Thomson W.T., Dahleh M.D., (1998) Theory of Vibration with Applications, 5th ed, Prentice Hall, New Jersey.
[13] Ewins DJ (2000) Modal testing: theory, practice and application, 2nd ed. Wiley, New York
[14] Guidelines for Evaluation of Marine Finite Element Analyses, SSC-475, Ship Structure Committee, 2019
[15] H.Ucar, "Ship Hull Girder Vibration", *Journal of Naval Science and Engineering*, Vol.7, No.1, pp. 1-21, 2011.
[16] World Meteorological Organization (WMO), International Codes, Volume I.1, Annex II to the WMO Technical Regulations, Part A - Alphanumeric Codes, 2011 ed., Updated in 2015.
[17] International Towing Tank Conference, "Technical Decisions and Recommendations", *12th ITTC*, Rome, Italy, 1969.
[18] K.A. Anıl, D.B. Danisman, K.Sarioz, "Simulation-based analysis of shipmotions in shor-cested irregular seas", Journal of ETA Maritime Science, 5 (1), pp. 19-38, 2017.